IEEE Access
Multidisciplinary ⋮ Rapid Review ⋮ Open Access Journal

Received 11 May 2024, accepted 12 August 2024, date of publication 14 August 2024, date of current version 27 August 2024.

Digital Object Identifier 10.1109/ACCESS.2024.3443471

RESEARCH ARTICLE

Optimal Multi-Microgrids Energy Management Through Information Gap Decision Theory and Tunicate Swarm Algorithm

REZA RASHIDI[1], ALIREZA HATAMI[1], MANSOUR MORADI[2], AND XIAODONG LIANG[3], (Senior Member, IEEE)

[1]Department of Electrical Engineering, Faculty of Engineering, Bu-Ali Sina University, Hamedan 65178-38695, Iran
[2]Department of Electrical Engineering, National University of Skills (NUS), Tehran 14357-61137, Iran
[3]Department of Electrical and Computer Engineering, University of Saskatchewan, Saskatoon, SK S7N 5A9, Canada

Corresponding author: Xiaodong Liang (xil659@mail.usask.ca)

ABSTRACT A multi-microgrid (MMG) consists of several individual microgrids (MGs) within a distribution system to improve the system's stability and reliability. A MMG can operate in grid-connected or island mode and requires advanced control techniques and effective energy management. This paper proposes a novel energy management approach for a MMG at the tertiary level control (TLC) using an adaptive optimal control model. Operational costs of the MMG are minimized for short-term planning while satisfying operational constraints of the network; the influential indices, the energy not supplied (ENS) and fatigue life (FL), remain balanced. The information gap decision theory (IGDT) is used to consider uncertainties in power generation and consumptions. MATLAB and DigSilent are used simultaneously to model optimally connected individual MGs within a MMG. The Tunicate Swarm Algorithm (TSA) is used for TLC for cost calculation and forming optimal connection models of individual MGs. The proposed method is validated through several case studies, showing superior performance.

INDEX TERMS Energy management, fatigue life, information gap decision theory, multi-microgrid, tertiary-level control, tunicate swarm algorithm.

ABBREVIATION

MG	Microgrid.
MMG	Multi-microgrid.
TSA	Tunicate swarm algorithm.
EV	Electric vehicle.
DR	Demand response.
DG	Distributed generation.
MT	Microturbine.
RER	Renewable energy resources.
RPC	Renewable power curtailment.
DER	Distributed energy resource.
PV	Photovoltaics.
ESS	Energy storage system.
WT	Wind turbine.
SW	Social welfare.
TLC	Tertiary-level control.
IGDT	Information gap decision theory.
PSO	Particle swarm optimization.
MAS	Multi-agent system.
AOCM	Adaptive optimal control model.
FL	Fatigue life.
CHP	Combined heat and power.
ENS	Energy not supplied (kWh).
PCC	Point of common coupling.
HV/NV/LV	High/Normal/Low-voltage.
Hf/Nf/Lf	High/Normal/Low-frequency.
P_{NL}	Nominal load power.
CRP	Cost reduction percentage.
MT_{cost}	The total cost of the microturbine ($).
MT^{EF}	The emission factor of MT (kg/kWh).
ENS_{cost}	The total cost of ENS ($).

The associate editor coordinating the review of this manuscript and approving it for publication was Mohsin Jamil.

$P_{loss_{Cost}}$	The total cost of losses ($).
MT_{cost}^{fuel}	The fuel cost of MT ($/kWh).
C_f	Fuel cost ($/Liter).
MT_{cost}^{op}	The operation cost of MT ($/kWh).
MT_{cost}^{MA}	The maintenance cost of MT ($/kWh).
MT_{cost}^{EM}	The emission cost of MT ($/kWh).
MT_{cost}^{FL}	The fatigue life cost of MT ($/kWh).
FL_K	FL coefficient.
γ	Fatigue rate.
P_{MT}	MT power (kW).
SOC	State of charge.
ρ	Air density (kg/m^3).
A	Wind generator blade area (m^2).
η^W	Wind generator power coefficient.
V_{WT}, V_{WT}^{nom}	Wind speed and nominal wind speed (m/s).
T, T_{amb}	Cell and environmental temperature of PV (°c).
N_{PVs}, N_{PVp}	Number of series and parallel cells in a PV module.
NOCT	Nominal operating cell temperature (°c).
G_T	Solar radiation on tilted module plane(kW/m^2).
τ	Power temperature coefficient.
P_d	The total load (kW).
$MAX\ P_d^{avg}$	The maximum supply of load.
P_{EV}	The total electric vehicle load (kW).
ζ	Radius of uncertainty.
P_c^t, P_{dis}^t	The total charging and discharging power at time t.
$P_{c,max}$, $P_{dis,max}$	The maximum charging and discharging power.
$P_{generation}^{min}$	The minimum power generation.
$P_{generation}^{max}$	The maximum power generation.
σ_{WT}	Scale parameter of the WT distribution.
$\alpha_{k_{t,s}}$	The beta distribution scale parameter of the solar index.
$\beta_{k_{t,s}}$	The beta distribution shape parameter of the solar index.
μ_{kt}, $\sigma_{k_{t,s}}^2$	The mean and variance values of the solar clearness index's historical data.
S_t	Remaining electricity in the shared ES at the time t.
η_c, η_{dis}	Charging and Discharging efficiencies of ES.
E_{rate}	The rated capacity of ES.
$f_{min,max,operation}$	Minimum, maximum, and operation frequency.
$V_{min,max,operation}$	Minimum, maximum, and operation voltage.
$\propto$	Non-essential load reduction factor.
N	The number of microgrids.
M	The number of generators in a microgrid.
K	The number of energy storage systems.
$F_{P,Q}^{max}$	The maximum active and reactive capacity of a line.

I. INTRODUCTION

Increasing penetration of distributed energy resources (DERs), including wind turbines (WTs), solar photovoltaic (PV) units, and energy storage systems (ESSs), in distribution systems introduces significant challenges for system planning and operation. Power generation is gradually transitioning from centralized generation facilities to DERs in modern power grids [1], [2].

Microgrids (MGs) are fundamental building blocks of a smart grid, and may include renewable and traditional distributed generation (DG) units, small power plants, combined heat and power (CHP) plants, and load [3]. MGs are mainly located near electrical loads and can operate in grid-connected or island mode. Among many operational aspects, the energy management system (EMS) for MGs is essential [4], significantly affecting their stability [5] and economic operations [6].

Energy management is studied for a grid-connected MG in [7], [8] and an islanded MG in [9]. A demand response (DR) model is proposed in [10] by sharing an EV parking station. In [11], the energy is managed through coordination and negotiation techniques among neighbors. In [12] and [13], the EV energy sharing and consumer participation have been studied simultaneously. However, a MG's capacity may not be sufficient to supply electrical load alone in certain operating conditions, which require forming a multi-microgrid (MMG) through connections with other MGs [14], [15], [16]. Boglou et al. have conducted the energy management of a MMG in [17]; the MMG formation has been optimized in terms of operating costs [18], stability [19], and protection [20].

There are three main control methods for MGs: centralized, decentralized, and distributed (Fig. 1). The centralized control offers a simple structure, low operating costs, and high speed, but may experience single-point failures [21]. The decentralized control has a more complex structure, and higher operating costs, but offers an acceptable reliability [22], [23]. The distributed control has the most complicated structure and is the most expensive for energy management in a MMG.

To manage energy in MGs without considering the energy not supplied (ENS) and fatigue life (FL), centralized control through machine learning is used to realize the optimal energy flow in [26]; the Internet of Things (IoT) and decentralized control are used in [28]; distributed control realized through the multi-agent system (MAS) and the game theory is proposed in [29]. In [27], ENS is considered, but FL is not.

The Information Gap Decision Theory (IGDT) is an efficient method for dealing with a high level of uncertainty [30]. The inability to supply load, especially sensitive load, increases operational costs directly related to ENS.

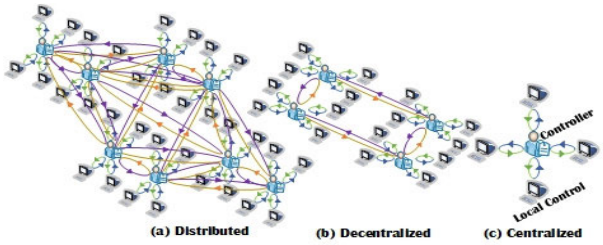

FIGURE 1. The structures of the three main control models: (a) distributed, (b) decentralized, (c) centralized.

By using IGDT, ENS is reduced, and operational costs are minimized.

In the literature, the primary purpose of energy management is to minimize costs, which can be in the form of electricity market exchange [31] to simultaneously increase profits of the consumer and the producer or reduce costs of power generation [32]. Objective functions include minimizing ENS, FL, and emission, and maximizing Social Welfare (SW). From the economic point of view, ENS and FL are the most influential factors in optimizing the MG's cost function. An optimal dispatch achieved by determining the power generation of each MG within a MMG reduces ENS and operational costs. FL depends on the power generation of each MG. When ENS is minimized, FL increases, and vice versa. Table 1 shows a summary of research done on the energy management of MMGs in the literature.

In this paper, we aim to determine the optimal connection of each MG within the MMG through the TLC to achieve a compromise between the two influential factors, ENS and FL, and optimize the cost function. Therefore, an adaptive optimal control model (AOCM) is proposed in this paper, through which power generation of each MG is firstly predicted, the optimal interconnection model of MGs is then determined using TLC by determining the consumption pattern by AOCM.

Real-life optimization problems have a large number of solution spaces with non-linear constraints, they are non-convex and complicated, leading to high computational costs. Metaheuristic algorithms are efficient for solving very complex optimization problems, and can be divided into two types, single solution-based algorithm (SSBA) and population-based algorithm (PBA). However, SSBAs cannot find the global optimum solution, and PBAs certainly can. PBAs can be further categorized based on the theory of evolutionary algorithms, logical behavior of physics algorithms, swarm intelligence of particles, and biological behavior of bio-inspired algorithms. The Tunicate Swarm Algorithm (TSA) is a new bio-inspired population-based metaheuristic algorithm, imitating jet propulsion and swarm behavior of tunicates in the navigation and foraging process [48]. TSA has been compared with other metaheuristic algorithms in [48], such as Genetic Algorithm (GA) and Particle Swarm Optimization (PSO), showing better solutions by providing global optimal solutions and good convergence, and thus, TSA is chosen in this paper.

The AOCM Rayleigh and Beta probability distribution for wind and solar output power are used to determine the generator's set-points and MGs connection models [33], and the computation time can be significantly reduced. The proposed method considers factors such as ENS, FL, and renewable power curtailment (RPC) and creates a balance among them in a MMG.

Increasing penetration of renewable energy sources creates operational challenges in power systems, often related to lack of capacities of the network model. To fill in this research gap, with the combination of two software, MATLAB and Digsilent, we propose a robust hierarchical control structure in this paper that can perform various operations, such as forming a MMG by connecting microgrids, reducing power output of diesel generators, and shedding load in a logical and fast manner. This control structure is functional very well thanks to accurate forecasting models of load and power generation, as well as the use of two powerful software tools simultaneously. The proposed model determines the best connection models of microgrids and optimal set points of generators at a desired level to minimize operating costs. This type of studies has not been done in the literature previously.

In this study, an optimal energy management method is proposed for MMGs at the tertiary level, and an intra-day scheduling is applied to minimize operating costs subjected to various operational constraints. Uncertainties in different resources and demands are managed using IGDT. The problem is solved by a two-stage iterative method using MATLAB and Digsilent: MATLAB first finds optimal connections between microgrids through TSA; the results from MATLAB are then input into Digsilent for load distribution, so that a high speed energy management structure of the MMG can be formed. Uncertainties are considered in this study to be compatible with the reality. The combined use of MATLAB and DigiSilent also leads to more accurate simulation results with less computation time.

In this paper, all load and power generation data are collected from actual one-year data samples within 24 hours for day-ahead load and generation forecasting. The main contributions of this paper include:

- A novel energy management approach for MMGs at TLC is proposed through IGDT and TSA. Using the AOCM framework, the daily load curves based on each MG's Arima model and generation resource capacity are prepared for TLC. The IGDT-TLC method manages uncertainties of load and power generation, and minimizes non-essential load shedding, ENS, and operational costs.
- The TSA algorithm chooses the best connection model for individual MGs by testing different connection models and adjusting each MG's local hierarchical control within a MMG.
- The simultaneous optimization through MATLAB for TLC implementation and through DigSilent for DG optimal dispatch in a MMG can be achieved.

TABLE 1. The research summary on MMGs.

Ref	Year	Objective	Grid specifications	Optimizer	communication		Component					Results
					Island	Connected	PV	WT	ESS	DG	EV	
[1]	2020	• Energy management for maximum use of RER. • Electric car charge management to reduce dependence on the utility grid.	IEEE 33-bus test system, Utility grid	Fmincon solver	---	✓	✓	✓	✓	×	✓	• Reduce power exchanges between the MG and utility grid. • Uncertainty and unavailability of the utility grid are not considered. • The FL factor for the generators in this study is not considered.
[6]	2021	• Optimal DR using a consumer participation incentive scheme. • Change the consumption pattern to shift the peak consumption time	1-MG, Utility grid	PSO-Fuzzy	---	✓	✓	✓	×	✓	×	• Change consumption patterns and optimize expected operating costs. • Uncertainty is not considered in the inability of the utility grid to supply MG's load and ENS factor.
[18]	2020	• Energy management is done to reduce operating costs. • Optimal operation of the energy storage system to increase system reliability.	4-MG, Utility grid	Shuffled complex evolution	---	✓	✓	✓	✓	✓	✓	• Using a comprehensive energy management strategy increases system reliability and reduces operating costs. • Factors related to FL are not considered.
[26]	2020	• Introducing a Rolling Time Horizon of energy management reduces power exchanges with the utility grid.	1-MG, Utility grid	Machine Learning	---	✓	✓	×	✓	×	×	• The battery storage system's management attempts to increase network quality and optimize energy management. • Loss and FL factors are not taken into account in the calculations.
[27]	2020	• Reduce power exchanges with the utility grid by introducing the Independence Performance Index. • Incentive scheme using Price Based Demand Response.	6-MG, Utility grid	Multi-Objective Decision Making	---	✓	✓	✓	✓	✓	×	• Reduce ENS and losses using stochastic compromise energy management programming. • The FL factor has not been investigated.
[29]	2021	• Distributed energy management using a Multi-Agent System.	1-MG, Utility grid	PSO- Game theory	---	✓	✓	✓	×	✓	×	• Cost optimization was obtained. • ENS, FL, and loss factors are not considered in the optimization.
[32]	2021	• An energy management strategy of a double-layer energy management system (EMS) is designed.	1-MG, Utility grid	Gurobi	---	✓	✓	✓	✓	×	×	• Long-term and short-term energy management is done in two different planning layers. • ENS, FL, and loss factors are not considered in the optimization.
[34]	2021	• Optimal operation using energy management in a microgrid. • Improvements in power losses and voltage deviations are investigated.	1-MG	Conditional value-at-credibility	✓	---	×	✓	×	✓	×	• Using compressed air energy storage, they control wind turbine oscillations. • ENS and FL (equipment useful life) are not considered. • Frequency is not included in the stability calculations.
[35]	2021	• Design blockchain technology implementation to reduce operating costs and improve power quality	IEEE 30-bus and 118-bus test systems	Type-2 fuzzy	✓	---	✓	✓	×	×	×	• Total profit is improved by using the proposed scheme. • ENS, FL, and loss factors are not considered in the optimization.
[36]	2021	• Investigating the effect of ESS and renewable energy scheduling on operating costs and social welfare.	IEEE 33-bus test system	PSO	---	✓	✓	✓	✓	✓	×	• Using Price-Based DR, the consumption pattern is shifted, reducing the operation cost.
This paper		• Load uncertainty, predicted by ARIMA and Adaptive Optimal Control Model structure. • Energy management to improve operating costs by considering ENS and FL factors simultaneously	A remote MMG with 6 MGs	TSA-IGDT	✓	✓	✓	✓	✓	✓	✓	• The challenge of sustainability constraints has been achieved without access to the utility grid. • Cost optimization was obtained. • All the factors required for optimization are considered.

The paper is arranged as follows: Section II describes the proposed energy management method for MMGs; the mathematical formulation of the proposed energy management method is derived in Section III; Case studies are conducted in Section IV; Section V concludes the paper and recommends the future work.

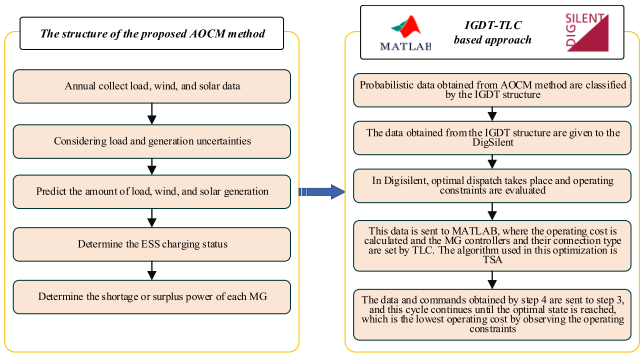

FIGURE 2. A graphical representation of the proposed method.

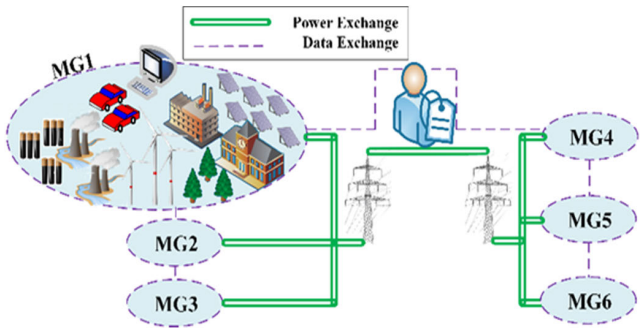

FIGURE 3. The structure of the test MMG network.

II. THE PROPOSED ENERGY MANAGEMENT METHOD FOR MMGS

In this paper, an effective IGDT and TSA-based optimal energy management approach is proposed for a MMG at TLC. The main idea is shown by the flowchart in Fig. 2, which can be implemented through a two-stage procedure as follows:

Stage 1: The proposed AOCM method can be implemented in the following five steps:

- *Step 1*: Data for the load, wind and solar resources are gathered on an annual basis.
- *Step 2*: Load and power generation uncertainties are considered.
- *Step 3*: Using the collected data in Step 1 and uncertainties in Step 2, predictions are made for the load, and the wind and solar power generation.
- *Step 4*: The charging status of the ESS is determined, i.e., whether the ESS should be charged or discharged based on the predicted load and power generation.
- *Step 5*: The power shortage/surplus for each MG is determined based on the predicted load and power generation.

Stage 2: The IGDT-TLC-based approach can be implemented in the following five steps:

- *Step 1*: The probabilistic data obtained from the AOCM method in Stage 1 are classified using the IGDT structure.
- *Step 2*: The data from the IGDT structure are sent from MATLAB to DigSilent.
- *Step 3*: In DigSilent, optimal dispatch of DGs is performed by satisfying operational constraints.
- *Step 4*: The data from DigSilent are sent back to MATLAB, where operational costs are calculated. The TLC optimization algorithm applies the proposed hierarchical control to each MG to minimize operational costs.
- *Step 5*: The data and commands obtained in Step 4 are sent back to DigSilent (Step 3), and this iterative cycle continues until the system reaches an optimal state to achieve the lowest operational cost while satisfying operational constraints.

In this paper, the test MMG network in Fig. 3 has two inter-connected sections without connecting to the utility grid. Each section has three MGs that share their resources to reduce operational costs. Power generation in each MG is controlled by the proposed local hierarchical controllers. These local hierarchical controllers are controlled through TLC, which is the central control of all MGs. TLC collects information, such as power generation prices, the grid status, and the usable resource capacity, from the MMG, performs connection among individual MGs, and, if necessary, reduces load through the DR program. There are essential and non-essential loads in this test MMG. If loads need to be reduced, non-essential loads participate in the DR program.

A. TLC STRUCTURE

There are three levels in the hierarchical control of a MMG: primary, secondary, and tertiary (Table 2). The primary level control has the highest control speed; primary controllers aim to control local loads and are located near the load. The secondary level control manages primary controllers. The TLC determines the working point of the secondary level control and manages energy to minimize operational costs.

B. IGDT

IGDT is suitable for a small number of data samples with severe uncertainties. In this paper, IGDT is used to manage uncertainties of power generation and load and reduce their probability range. With IGDT, the initial data are firstly obtained using accurate models of power generation and load, and uncertainties of the data are considered using probabilistic methods, such as Rayleigh and Beta probability distribution.

III. THE MATHEMATICAL FORMULATION OF THE PROPOSED METHOD

The mathematical formulation of the objective function and its associated constraints of the proposed method are presented in Eqs. (1) to (25), $i = 1, \ldots, N$, $j = 1, \ldots, M$, $t = 1, \ldots, T$. Eq. (1) shows the total cost of a MMG, including costs of MTs, WTs, PVs, ESSs, ENS, and power losses. The cost of MTs is presented in (2) to (7). Eq. (5) is related to the greenhouse gas emission from MTs under the Paris Agreement [37], [44]. Eq. (6) represents the cost of FL, where γ is the fatigue rate (Fig. 4), and γ increases as power

TABLE 2. Three levels in the hierarchical control of a MMG [47].

Control level	Duty	Performance time	Optimization method
Tertiary	Determine the set points of secondary control Energy management optimization	Seconds to minutes	MAS MPC
Secondary	Determine the set points of primary control Voltage and frequency and other constraints restoration	100 ms to 1 s	MAS MPC Fuzzy Primary-Secondary
Primary	Sustainability of local resources	0.1 ms to 10 ms	Droop

generation increases.

$$Min\ Cost = Min\Big[MT_{cost} + WT_{cost} + PV_{cost} + ESS_{cost} + ENS_{cost} + P_{Cost}^{loss}\Big] \quad (1)$$

$$MT_{cost} = \sum_{i=1}^{N_{MG}} \sum_{j=1}^{N_{MT}(i)} \sum_{t=1}^{T} \Big[MT_{cost}^{fuel}(i,j,t) + MT_{cost}^{OP}(i,j,t) + MT_{cost}^{MA}(i,j,t) + MT_{cost}^{EM}(i,j,t) + MT_{cost}^{FL}(i,j,t)\Big] \quad (2)$$

$$MT_{cost}^{OP}(i,j,t) = P_{MT}(i,j,t) \times Cost_{op}^{MT}(i,j,t) \quad (3)$$

$$MT_{cost}^{MA}(i,j,t) = P_{MT}(i,j,t) \times Cos_{MA}^{MT}(i,j,t) \quad (4)$$

$$MT_{cost}^{EM}(i,j,t) = (C_E \times P_{MT}(i,j,t) \times MT_{CO_2}^{EF}) + (C_E \times P_{MT}(i,j,t) \times MT_{NO_X}^{EF}) + (C_E \times P_{MT}(i,j,t) \times MT_{SO_2}^{EF}) \quad (5)$$

$$MT_{cost}^{FL}(i,j,t) = FL_K \times \varphi_{MT}(i,j,t) \times \gamma \times P_{MT}(i,j,t) \quad (6)$$

$$\varphi_{MT}(i,j,t) = MT_{cost}^{OP}(i,j,t) + MT_{cost}^{MA}(i,j,t) + MT_{cost}^{EM}(i,j,t) \quad (7)$$

$$WT_{cost} = \sum_{i=1}^{N} \sum_{j=1}^{M} \sum_{t=1}^{T} \Big[WT_{cost}^{OP}(i,j,t) + WT_{cost}^{MA}(i,j,t) + WT_{cost}^{FL}(i,j,t)\Big] \quad (8)$$

$$WT_{cost}^{OP}(i,j,t) = P_{WT}(i,j,t) \times Cost_{op}^{WT}(i,j,t) \quad (9)$$

$$WT_{cost}^{MA}(i,j,t) = P_{WT}(i,j,t) \times Cost_{MA}^{WT}(i,j,t) \quad (10)$$

$$WT_{cost}^{FL}(i,j,t) = FL_K \times \varphi_{WT}(i,j,t) \times \gamma \times P_{WT}(i,j,t) \quad (11)$$

$$\varphi_{WT}(i,j,t) = WT_{cost}^{OP}(i,j,t) + WT_{cost}^{MA}(i,j,t) \quad (12)$$

$$PV_{cost} = \sum_{i=1}^{N_{MG}} \sum_{j=1}^{N_{PV}(i)} \sum_{t=1}^{T} \Big[PV_{cost}^{OP}(i,j,t) + PV_{cost}^{MA}(i,j,t) + PV_{cost}^{FL}(i,j,t)\Big] \quad (13)$$

$$PV_{cost}^{OP}(i,j,t) = P_{PV}(i,j,t) \times Cost_{op}^{PV}(i,j,t) \quad (14)$$

$$PV_{cost}^{MA}(i,j,t) = P_{PV}(i,j,t) \times Cost_{MA}^{PV}(i,j,t) \quad (15)$$

$$PV_{cost}^{FL}(i,j,t) = FL_K \times \varphi_{PV}(i,j,t) \times \gamma \times P_{PV}(i,j,t) \quad (16)$$

$$\varphi_{PV}(i,j,t) = PV_{cost}^{OP}(i,j,t) + PV_{cost}^{MA}(i,j,t) \quad (17)$$

$$ESS_{cost} = \sum_{i=1}^{N_{MG}} \sum_{j=1}^{N_{ESS}(i)} \sum_{t=1}^{T} \Big[ESS_{cost}^{OP}(i,j,t) + ESS_{cost}^{MA}(i,j,t) + ESS_{cost}^{FL}(i,j,t)\Big] \quad (18)$$

$$ESS_{cost}^{OP}(i,j,t) = P_{ESS}(i,j,t) \times Cost_{op}^{ESS}(i,j,t) \quad (19)$$

$$ESS_{cost}^{MA}(i,j,t) = P_{ESS}(i,j,t) \times Cost_{MA}^{ESS}(i,j,t) \quad (20)$$

$$ESS_{cost}^{FL}(i,j,t) = FL_K \times \varphi_{ESS}(i,j,t) \times \gamma \times P_{ESS}(i,j,t) \quad (21)$$

$$\varphi_{ESS}(i,j,t) = ESS_{cost}^{OP}(i,j,t) + ESS_{cost}^{MA}(i,j,t) \quad (22)$$

$$ENS_{cost} = \sum_{i=1}^{N_{MG}} \sum_{j=1}^{M} \sum_{t=1}^{T} ENS_k \times £(i,j,t) \times DurationENS(i,t) \quad (23)$$

$$£(i,j,t) = DG_{cost}^{OP}(i,j,t) + DG_{cost}^{MA}(i,j,t) \quad (24)$$

$$P_{Cost}^{loss} = \sum_{i=1}^{N_{MG}} \sum_{j=1}^{M} \sum_{t=1}^{T} P_{loss}(i,j,t) \times Cost_{loss} \quad (25)$$

Costs of WTs, PVs, and ESSs are described in (8) to (22). There are no costs associated with fuel and emissions. Eq. (23) shows the cost of ENS, where the £ factor is the highest cost factor of power generation due to load shedding, i.e., £ is a penalty factor that imposes a high cost on the cost function when the MMG has load shedding. Eq. (25) is the cost of power losses.

A. RENEWABLE POWER GENERATION

The power output of a WT is given as follows [38]:

$$P_{WT}(t) = 0.5 \times \rho \times A \times \eta^{W} \times min(V_{WT}(t), V_{WT}^{nom})^3 \quad (26)$$

$$V_{WT}^{Cut\ in} \le V_{WT}(t) \le V_{WT}^{Cut\ out} \quad (27)$$

The power output of a PV system is given as follows [39]:

$$P_{PV}(t) = [P_{PV_{STC}} \times (\frac{G_T(t)}{1000}) \times [1 - \tau \times (T(t) - 25)]] \times N_{PVs} \times N_{PVp} \quad (28)$$

$$T(t) = T_{amp} + (\frac{G_T(t)}{800}) \times (NOCT - 20) \quad (29)$$

Eq. (30) is based on IGDT to reduce uncertainties in renewable power generation.

$$\text{Max } P_{RES}^{avg} = \sum_{i=1}^{N_{MG}} (P_{RES}) \times (1 + \zeta) \quad (30)$$

B. ENERGY STORAGE SYSTEM

The ESS is modeled as follows:

$$SOC_t = \frac{S_t}{E_{rate}} \quad (31)$$

$$SOC^{min}(i,j) \le SOC_t(i,j,t) \le SOC^{max}(i,j)\ where\ i = 1,\ldots,N, j = 1,\ldots,K, t = 1,\ldots,T \quad (32)$$

$$P_c^t = \sum_{i=1}^{m} P_{c,i}^t \quad (33)$$

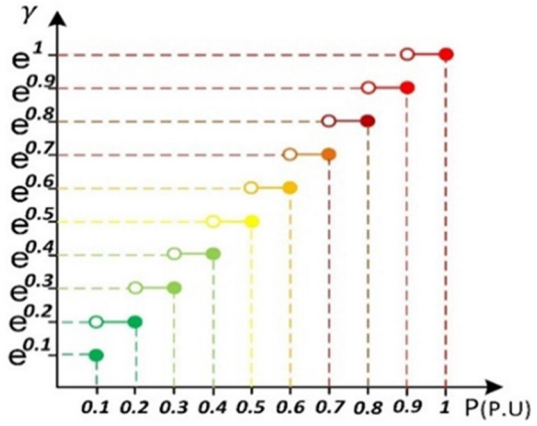

FIGURE 4. The fatigue rate for power generation.

$$P_{dis}^{t} = \sum_{i=1}^{m} P_{dis,i}^{t} \tag{34}$$

$$P_{c,i}^{t} P_{dis,i}^{t} = 0 \tag{35}$$

$$-P_{c,max} \le P_t \le P_{dis,max} \tag{36}$$

$$S_t = S_{t-1} + P_c^{t-1}\eta_c \Delta t - \frac{P_{dis}^{t-1}\Delta t}{\eta_{dis}} \tag{37}$$

$$S_1 = S_T \tag{38}$$

Eqs. (31) and (32) show the charge status and their constraints. Eqs. (33) to (36) show each MG's charge and discharge power. Eqs. (37) and (38) introduce each MG's shareable power.

C. MICROTURBINES

MTs use fossil fuels and have emissions. Eq. (39) provides power generation limits for MTs. Eq. (40) shows the relation between fuel costs and the output power of a MT [41], where a_i, b_i and C_i are cost coefficients of the MT.

$$P_{MT}^{min}(i,j) \le P_{MT}(i,j,t) \le P_{MT}^{max}(i,j) \quad i = 1,2,\ldots,N_{MG} j = 1,2,\ldots,N_{MT}(i), \quad t = 1,2,\ldots,T \tag{39}$$

$$MT_{cost}^{fuel} = \sum_{i=1}^{N_{MG}} \sum_{j=1}^{N_{MT}(i)} \sum_{t=1}^{T} C_f \times \left[a_i P_{MT}^2(i,t) + b_i P_{MT}(i,t) + C_i\right] (\$/hr) \tag{40}$$

D. THE LOAD UNCERTAINTY MODEL

Uncertainties of the load are expressed in (41) by the probability density function (PDF). In this model, the normal distribution shows good accuracy, where μ and σ represent the mean and the variance, respectively. Eq. (42) is to minimize load shedding based on IGDT.

$$P_d + P_{EV} = \frac{1}{\sigma_{est}\sqrt{2\pi}} e^{-\frac{(x-\mu_{est})^2}{2\sigma_{est}^2}} \tag{41}$$

$$\text{Max } P_d^{avg} = \sum_{i=1}^{N_{MG}} (P_d + P_{EV}) \times (1+\zeta) \tag{42}$$

E. UNCERTAINTIES OF RENEWABLE POWER GENERATION

Uncertainties of wind power generation are represented by the Rayleigh probability distribution [42]:

$$P_{WT} = \frac{V}{\sigma_{WT}^2} e^{\frac{-V^2}{2\sigma_{WT}^2}} \tag{43}$$

Uncertainties of solar PV power generation are represented by the Beta probability distribution [43]:

$$P_{PV} = \left(\frac{1}{B(\alpha,\beta)}\right) K_{t,s}^{\alpha-1}(1-K_{t,s}) \tag{44}$$

$$\alpha_{k_{t,s}} = \left(\frac{(1-\mu_{kt})}{\sigma_{k_{t,s}}^2} - \frac{1}{\mu_{k_{t,s}}}\right)\mu_{k_{t,s}}^2 \tag{45}$$

$$\beta_{k_{t,s}} = \alpha_{k_{ts}}\left(\frac{1}{\mu_{k_{t,s}}} - 1\right) \tag{46}$$

F. OTHER CONSTRAINTS TO MAINTAIN THE STABILITY OF MMGS

Other constraints include:

$$\sum_{i=1}^{N_{MG}} [P_i^{PV} + P_i^{WT} + P_i^{MT} + P_i^{Dis/ESS}] = \sum_{i=1}^{N_{MG}} (P_d + P_{EV} + P_i^{C/ESS}) \tag{47}$$

$$f_{min} \le f_{operation} \le f_{max} \tag{48}$$

$$V_{min} \le V_{operation} \le V_{max} \tag{49}$$

$$\begin{aligned} &Total\ generation\ capacity \\ &\quad \ge Total\ essential\ loads \\ &\quad + \propto \times (Total\ non-essential\ loads) \\ &\quad + Losses\ 0 \le \propto \le 1 \end{aligned} \tag{50}$$

Eqs. (47) to (50) show a balance of power generation and load to maintain the stability of the MMG. In DigSilent, the optimal load dispatch is performed using Newton-Raphson load distribution equations as follows:

$$S_i^* = V_i^* I_i = P_i - jQ_i \tag{51}$$

$$P_i = P_{Gi} - P_{Di} \tag{52}$$

$$Q_i = Q_{Gi} - Q_{Di} \tag{53}$$

where S_i is the apparent power of each node. P_{Di} and Q_{Di} are active and reactive power consumed, P_{Gi} and Q_{Gi} are active and reactive power generated in each node, respectively. The allowable power capacity range of a line can be determined by

$$|F_{P,Q}| \le F_{P,Q}^{max} \tag{54}$$

G. SPECIFICATIONS OF THE TSA ALGORITHM

The mathematical modeling of TSA has three primary conditions: avoid conflicts between search agents, move towards the position of the best search agent, and be close to the best search agent [48]. To prevent conflicts between search agents, the $\vec{A}$ vector is used to calculate the position of the new search agent as follows:

$$\vec{A} = \frac{\vec{G}}{\vec{M}} \tag{55}$$

$$\vec{G} = c_2 + c_3 - \vec{F} \quad (56)$$

$$\vec{F} = 2 \times c_1 \quad (57)$$

where $\vec{G}$ is the gravity force and $\vec{F}$ shows the water flow direction in the deep ocean. The variables, c_1, c_2, and c_3, are random numbers in the range of [1, 0]. $\vec{M}$ is the social force between search agents, which can be calculated as follows:

$$\vec{M} = [P_{min} + c_1.P_{max} - P_{min}] \quad (58)$$

where P_{min} and P_{max} are initial and subordinate speeds for social interaction, respectively. In this paper, $P_{min} = 1, and\ P_{max} = 4$. The three vectors, $\vec{A}$, $\vec{G}$, and $\vec{F}$, assist the solutions to behave randomly in a given search space, are responsible for avoiding conflicts between different search agents, and provide possibility of better exploration and exploitation phases through variations in the three vectors [48].

The TSA algorithm in problem-solving can be summarized as follows:

- *Step 1*: Initialize the tunicate population.
- *Step 2*: Choose initial parameters and the maximum number of iterations.
- *Step 3*: Calculate the fitness value of each search agent.
- *Step 4*: The best search agent is explored in the given search space.
- *Step 5*: Update the position of each search agent.
- *Step 6*: Adjust the updated search agent, which goes beyond the boundary in a given search space.
- *Step 7*: Compute the updated search agent's fitness value, then update the tunicate population.
- *Step 8*: The algorithm stops if the stopping criterion is satisfied. Otherwise, repeat Steps 5–8.
- *Step 9*: Return the best optimal solution obtained.

The computational efficiency, time and space complexity of the proposed TSA algorithm are explained as follows [48]:

- *Computational Efficiency:* Computational efficiency indicates the algorithm's performance through computational time. In [48], the average computational time performed by Harris Hawks optimization (HHO), PSO, equilibrium optimizer (EO), Salp swarm algorithm (SSA), grey wolf optimizer (GWO), and TSA are compared for 30 independent executions in 23 benchmark functions, and their computational time are 0.17945 s, 0.10355 s, 0.098161 s, 0.092174 s, 0.076043 s, and 0.071683 s, respectively. The TSA uses the least amount of computational time among these algorithms, showing a superior computational efficiency.
- *Time complexity:* The initialization process of the population needs $\mathbb{O}(n \times d)$ time, where n is the population size, and d is the dimension of a given test problem; the agent fitness needs $\mathbb{O}(Max_{iterations} \times n \times d)$ time, where $Max_{iterations}$ is the maximum number of iterations; TSA needs $\mathbb{O}(N)$ time, where N defines the jet propulsion and swarm behaviors of tunicate for better exploration and exploitation. Therefore, the total time complexity of the TSA algorithm is $\mathbb{O}(Max_{iterations} \times n \times d \times N)$.

TABLE 3. Possible actions based on the IGDT-TLC approach.

	N	
Action in MG_i^N	*Lf NV/Nf LV/Lf LV*	*Hf NV/Nf HV/HfHV*
RER curtailment	×	✓
Load shedding	✓	×
MT power increase	✓	×
MT power decrease	×	✓
Importing power	✓	×
Exporting power	×	✓
ESS charging	×	✓
ESS discharging	✓	×

- *Space complexity:* The space complexity of the TSA algorithm is $\mathbb{O}(n \times d)$, which is considered as the maximum amount of space during its initialization process."

IV. CASE STUDIES

To validate the proposed energy management method in a MMG, case studies are conducted using the test MMG network in Fig. 3. The detailed configuration of the test MMG network is shown in Fig. 5, with six MGs divided into two inter-connected regions. The six MGs can exchange power without connecting to the utility grid. The power generation and ESSs in the test MMG in Fig. 5 include:

- Six WTs, each located in one MG (Three WTs are rated at 20 kW each, and other three WTs are rated at 30 kW each).
- Six PV units, each located in one MG (five PV units are rated at 20 kW each, and one PV unit is rated at 10 kW).
- Six ESSs, each located in one MG (two ESSs are rated at 8 kW each, two ESSs are rated at 10 kW each, and two ESSs are rated at 12 kW each).
- Six MTs, each located in one MG (two MTs are rated at 50 kW each, two MTs are rated at 40 kW each, one MT is rated at 60 kW, and one MT is rated at 70 kW).

In Fig. 5, the load and transmission lines are present in each MG. The load consists of industrial, health services, residential & EV, official, and military, and the capacity of each type of load in kW are given in Fig. 5. The impedance and length of each transmission line are also given in Fig. 5.

For wind power generation, the Rayleigh probability distribution and the data from the Kiata wind farm in Australia are used [45]. For solar power generation, German Krebse PV solar farm data from [46] are used. The detailed data for the system in Fig. 5 are given in Table 4.

Figs. 6 and 7 show power generation by WT and PV, respectively. Given the capacity of resources, Fig. 8 shows the daily load curve of each MG in the test MMG. The power of ESS participation in the MMG is shown in Fig. 9.

The set of commands generated from the IGDT-TLC has the logic in Table 3, where the TLC issues orders that improve stability and reduce operational costs. Table 4 shows the load and power generation data.

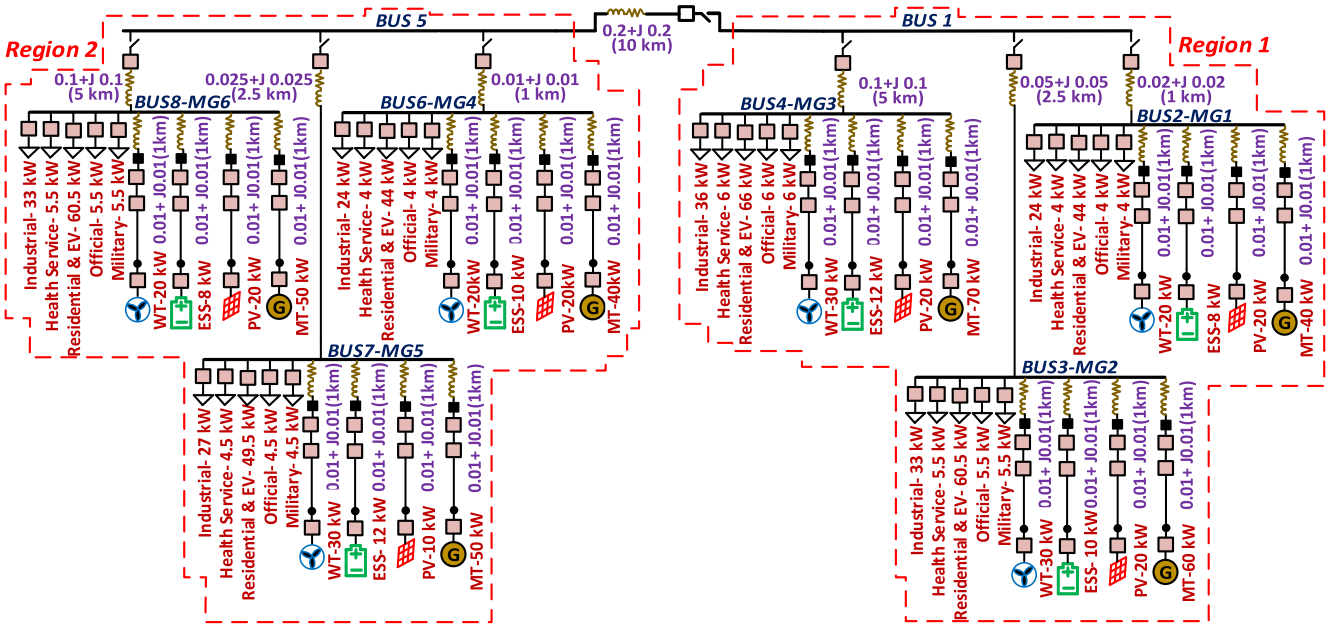

FIGURE 5. Specifications of the proposed MMG test network.

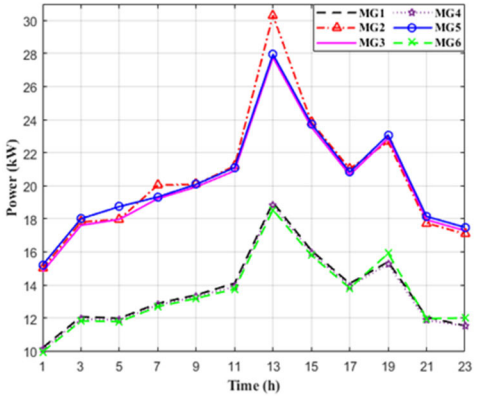

FIGURE 6. WT 24-hour power generation in each MG.

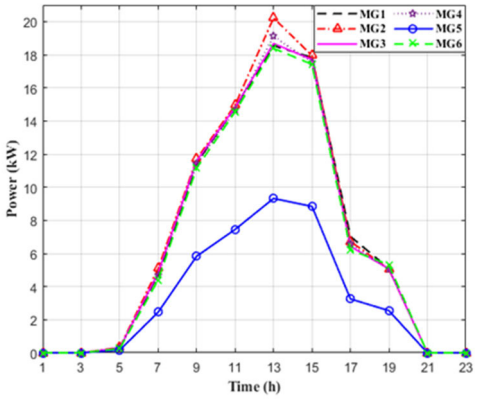

FIGURE 7. PV 24-hour power generation in each MG.

The optimization through TSA involves a multi-objective function consisting of linear and mixed-integer non-linear programming. To solve this problem, MATLAB 2019b and DigSilent 15.1.7 are used simultaneously: MATLAB optimizes the connection of MGs and TLC commands, and DigSilent performs optimal dispatch of DGs. It is conducted on a computer with Core i7, 1 GHz processor, and 4 GB of RAM.

The objective in the test MMG is to minimize the renewable power generation curtailment (RPC), ENS and FL simultaneously, which directly affect the cost function. It is assumed that renewable power generation from WTs and PVs is used to the maximum while trying to reduce MTs' usage.

In this paper, five case studies are conducted under different power generation and loads. The acceptable voltage and frequency limits are assumed to be 1 ± 0.05 per unit and 50 ± 0.02 Hz, respectively. Cases 1-4 are under the AOCM framework using the IGDT-TLC method. Case 5 considers the MT failure in the control process.

A. CASE 1: POWER SHORTAGE IN SOME MGS

In Case 1a at 17 o'clock, RERs generate 139.44 kW. Due to power shortages in MGs 3 and 6, operational constraints for the voltage and frequency are not within acceptable limits. To correct this, the DR program must reduce the load by 2.453 kW. A MMG is formed by MGs 3, 4, 5, and 6 (50 Hz nominal frequency) with a voltage of 0.9594 p.u. at the interconnection bus, and the DR program is not needed. Transmission losses increase by 0.744 kW, the FL factor decreases by \$4.363, and the CRP index decreases by 21.029%.

TABLE 4. Data of load and generation in the test MMG [37], [44], [47].

	Load and power generation characteristics								
	Nominal load (kW)					*Generations (kW)*			
MG_i	*Industrial*	*Health Service*	*Residential & EV*	*Official*	*Military*	*WT*	*PV*	*MT*	*ESS*
MG_1	24	4	44	4	4	20	20	40	10
MG_2	33	5.5	60.5	5.5	5.5	30	20	60	10
MG_3	36	6	66	6	6	30	20	70	12
MG_4	24	4	44	4	4	20	20	40	10
MG_5	27	4.5	49.5	4.5	4.5	30	10	50	12
MG_6	33	5.5	60.5	5.5	5.5	20	20	50	8

Components	*Parameters*
MT	*Cost coefficients: a= 0.011, b= 0.1757, c= 1.6153 and* C_f *= 0.9 \$/L.* $Cost_{MA}^{MT}$ *= 0.0125 \$/kWh,* $Cost_{op}^{MT}$ *= 0.01312 \$/kWh,* C_E *=0.04 kg/kWh,* $MT_{CO_2}^{EF}$ *= 0.76 kg/kWh,* $MT_{NO_X}^{EF}$ *=0.00455kg/kWh.* FL_K *= 0.02.*
WT	$Cost_{MA}^{WT}$ *= 0.08 cent/ kWh,* $Cost_{OP}^{WT}$ *= 0.084 cent/ kWh,* FL_K *= 0.02.*
PV	$Cost_{MA}^{PV}$ *= 0.09 cent/ kWh,* $Cost_{OP}^{PV}$ *= 0.0945 cent/ kWh.*
ESS	$Cost_{MA}^{ESS}$ *= 0.03 cent/ kWh,* $Cost_{OP}^{PV}$ *= 0.0315 cent/ kWh.*
Other	ENS_k *= 1.5,* £ *= 0.02562 \$/kWh,* $loss_{Cost}$ *= 0.04 \$/kWh.*

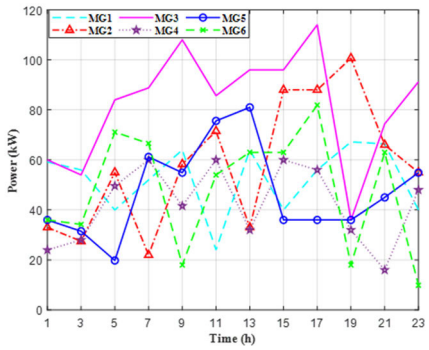

FIGURE 8. Forecasted loads of each MG in the test MMG.

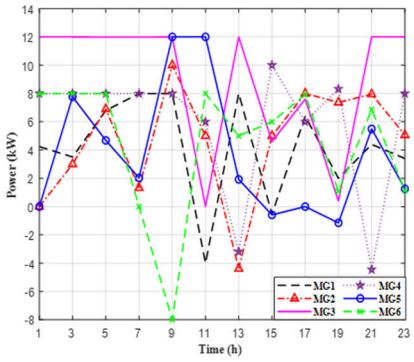

FIGURE 9. ESS power participation rate in each MG.

In Case 1b at 21 o'clock, MG_1 faces a power shortage and must participate in the DR program by reducing non-essential loads by 6.5129 kW. PVs have no power output and active power from renewable energy sources, P_{RER}, is 89.704 kW. Using the proposed control method by connecting and controlling MGs 1, 2, 4, and 6, the TLC sets operational constraints within an allowable range without participating in the DR program. Transmission losses increase by 0.172 kW, the FL factor is reduced to \$0.983, and the CRP index decreases by 39.128%. Comparing to Case 1a, the power shortage increases in Case 1b without solar PV power generation, and the TLC's performance becomes more prominent. EMS programming tries to use the maximum amount of RERs.

B. CASE 2: POWER SHURPLUS IN SOME MGS

In Case 2a at 13 o'clock, MGs 2 and 4 have 7.538 kW and 1.59 kW of renewable power generation surplus, respectively, which leads to their instability and, thus, must be curtailed. The surplus renewable power can reduce operational costs if used by other MGs. TLC takes advantage of the surplus power by connecting MGs 2, 4, 5, and 6. Transmission losses increase from 2.173 kW to 4.678 kW, the FL factor drops from \$8.225 to \$4.414, and the CRP index decreases by 10.638%.

In Case 2b at 23 o'clock, MG_6 has a power surplus of 2.475 kW, causing its frequency to increase to 50.951 Hz, which must be reduced. The voltage is within the allowable range. The operational cost is \$74.302. By connecting MGs 2, 3, 5, and 6, TLC ensures the frequency within an allowable range. The FL factor decreases from \$18.131 to \$14.202, and the operational cost is \$69.351 with the CRP index of 6.663%. Comparing to Case 2b, the optimization in Case 2a with more RPC value increases the CRP index.

C. CASE 3: SIMULTANEOUS POWER SHORTAGE AND POWER SURPLUS IN SOME MGS

In Case 3 at 19 o'clock, MG_1 has a power shortage and MG_6 has a power surplus. To maintain stability, MG_1 must participate in the DR program and reduce 3.271 kW of non-essential loads while MG_6 must reduce RER power by 2.784 kW. The operational cost is \$75.558. By connecting MGs 1, 2, 3, 5, and 6, TLC ensures the frequency of MG_1 and MG_6 remains at 50 Hz. Transmission power losses increase by 1.743 kW, but there is no need to participate in the DR program (ENS =

TABLE 5. The status of MGs before and after using the proposed model.

	Event	Power shortage			Power surplus			Power shortage / surplus		Normal	MT failure
	Cases	Case 1a		Case 1b	Case 2a		Case 2b	Case 3		Case 4	Case 5
Initial condition	Hour	**17**		**21**	**13**		**23**	**19**		**3**	**9**
	Problem MG_i	MG_3	MG_6	MG_1	MG_2	MG_4	MG_6	MG_1	MG_6	×	MG_4
	V (Volt)	0.9473	0.9656	0.94689	1.0901	1.0918	1.005	0.976	1.017	0.99	0.986
	f (Hz)	49.921	49.977	49.568	50.87	50.22	50.951	49.792	50.594	50	49.188
	RPC (kW)	0	0	0	7.538	1.59	2.475	0	2.784	0	0
	V&F status	Lv / Lf		Lv / Lf	Hv / Hf		Nv / Hf	Nv / Lf / Hf		Nv / Nf	Nv / Lf
	P_{NL} (kW)	431.9		330.8	369		299	289.85		231.2	344.8
	ESS ^{T}(kW)	35.95		32.2472	19.327		30.916	18.011		42.2717	42
	MT^T_{POWER} (kW)	243.681		202.923	112.634		179.764	126.728		97.45	123.766
	ENS^T (kW)	2.453		6.5129	0		0	3.271		0	7.997
	P_{RER} (Kw)	139.444		89.704	247.216		86.889	143.001		89.031	164.496
	Losses^T(Kw)	3.0788		3.22	2.173		1.694	1.674		0.868	2.195
	ENS^T_{Cost} ($)	15.417		34.083	0		0	10.6902		0	25.5248
	FL^T_{Cost} ($)	33.153		20.003	8.225		18.131	15.8		5.749	13.289
	OP^T_{Cost} ($)	132.84		133.94	47.816		74.302	75.558		40.196	100.39

	MGs participant	$MGs_{3,4,5,6}$		$MGs_{1,2,4,6}$	$MGs_{2,4,5,6}$		$MGs_{2,3,5,6}$	$MGs_{1,2,3,5,6}$		$MGs_{1,4,5,6}$				$MGs_{4,6}$	
After Using the proposed method	Improved MG_i	MG_3	MG_6	MG_1	MG_2	MG_4	MG_6	MG_1	MG_6	MG_1	MG_4	MG_5	MG_6	MG_4	MG_6
	V (volt)	0.9594	0.9721	0.9541	0.994	0.982	0.996	0.9723	0.994	0.975	0.99	0.991	0.99	1.05	1.05
	f (Hz)	50	50	50	50	50	50	50	50	50	50	50	50	50.011	50.011
	P_{Im}	✓	✓	✓	×	×	×	✓	×	✓	×	×	×	✓	×
	P_{Ex}	×	×	×	✓	✓	✓	×	✓	×	✓	✓	✓	×	✓
	V&F status	NV / NF		NV / NF	NV / NF		NV / NF	NV / NF		NV / NF				NV / NF	
	ESS ^{T}(kW)	36.05		32.2472	19.751		30.869	18.034		42.2717				42.08	
	MT^T_{POWER} (kW)	247.605		203.201	103.17		177.372	126.413		99.108				138.7	
	P_{RER} (Kw)	139.444		89.704	242.027		86.414	142.381		89.031				155.951	
	Losses^T(Kw)	3.8233		3.3925	4.678		2	3.417		2.645				2.401	
	FL^T_{Cost}($)	28.79		19.02	4.414		14.202	11.586		3.302				13.088	
	OP^T_{Cost}($)	104.91		81.534	42.729		69.351	55.349		37.602				59.756	
	CRP %	21.029		39.128	10.638		6.663	26.746		6.455				40.475	

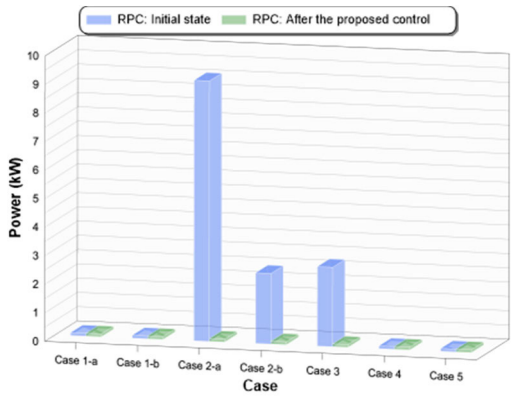

FIGURE 10. The RPC factor in 24-hour.

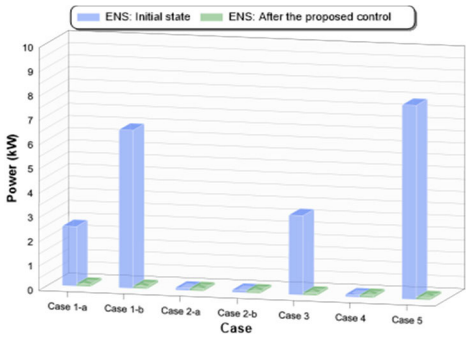

FIGURE 11. ENS factors in 24-hour.

0 kW). The FL factor decreases from \$15.8 to \$11.586, and the CRP index decreases by 26.746%.

D. CASE 4: MGS IN POWER EQUILIBRIUM (NO POWER SHORTAGE OR SHURPLUS)

Case 4 at 3 o'clock shows a power-balanced condition for MGs with an average voltage of 0.99 p.u. and a frequency of 50 Hz. The operational cost is \$40.196. Using the proposed method, TLC establishes a relationship among MGs 1, 4, 5, and 6 while maintaining operational constraints within the allowable range. Transmission losses increase from 0.868 kW to 2.645 kW, the FL factor is reduced from \$5.749 to \$3.302, and the CRP index is 6.455%.

E. CASE 5: MT FAILURES

In Case 5 at 9 o'clock, the MT in MG_4 fails and is out of service. Due to the power shortage in MG_4, the frequency drops to 49.188 Hz, and the DR program participation is

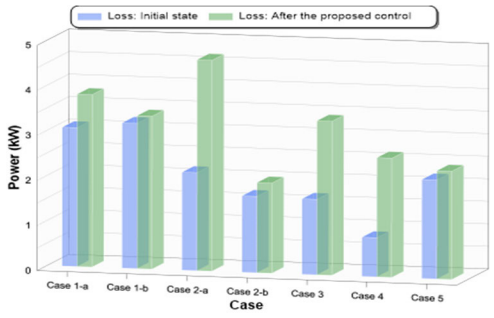

FIGURE 12. Losses in 24-hour.

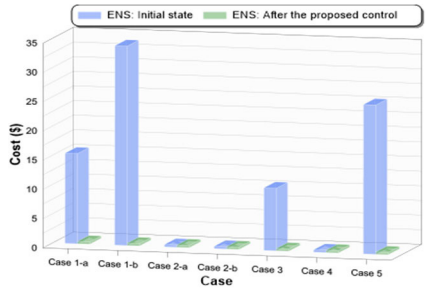

FIGURE 13. ENS costs in 24-hour.

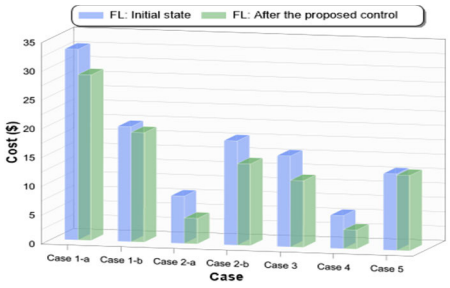

FIGURE 14. FL costs in 24-hour.

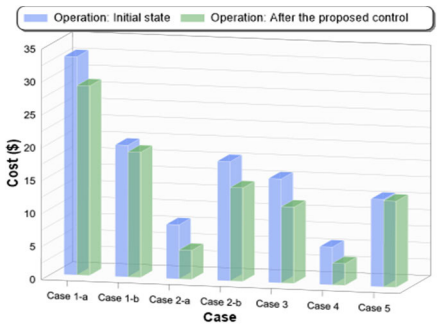

FIGURE 15. Operation costs in 24-hour.

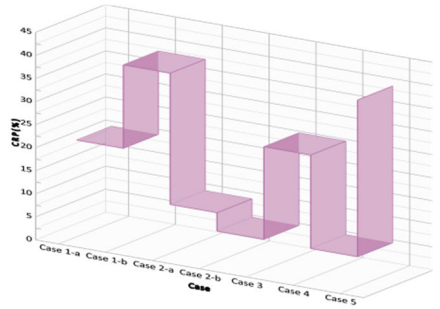

FIGURE 16. CRP in different cases.

required by reducing non-essential loads of 7.997 kW. The operating cost is $100.39. TLC examines connections of MGs with the lowest power generation level and MG_6 is found with its MT power generation equal to 1.794% of its nominal capacity. By connecting MG_4 and MG_6, TLC increases the system frequency to 50.011 Hz, which is within the allowable range, and the DR program participation is not required. Transmission losses increase by only 0.206 kW, and the CRP index is 40.475%.

Table 5 shows the result summary of the five case studies. Fig. 10 shows the RPC factor during 24 hours. The RPC factor is minimized with the proper control when the RER is high. MGs often face power shortages, and ENS is used to represent such power shortages. In Fig. 11, the highest ENS occurs at 9 o'clock because at this time, MT-MG_4 is out of service. A high ENS also occurs at 21 o'clock due to lack of solar PV power generation. One issue regarding power exchange in a MMG is the increased power losses, and TLC tries to form a MMG with the least power losses. In Fig. 12, power losses in Case 4 are more than three times their initial value. Four MGs in both regions of the test MMG network are connected, and the CRP index is equal to 6.455%.

Costs of ENS are shown in Fig. 13. A comparison between Figs. 13 and 14 indicates that TLC has tried to maintain both ENS and FL at an acceptable level. Fig. 15 shows operational costs before and after optimization. The CRP index based on the percentage of optimization is shown in Fig. 16.

V. CONCLUSION AND FUTURE WORK

This paper proposes a novel multi-objective energy management system for MMGs through Information Gap Decision Theory and Tunicate Swarm Algorithm to minimize operational costs and improve system stability. The proposed EMS uses an adaptive optimal control framework at the tertiary level control to maximize the control system's adaptability by considering uncertainties of load and power generation. IGDT handles uncertainties by increasing the probability of occurrence in forecasts. Multi-objectives refer to ENS, FL, and transmission line losses. TLC reduces ENS to optimize operational costs, causing FL to increase; to reduce FL, the load must be reduced, causing ENS to increase. MATLAB and DigSilent are used simultaneously in the MMG control process for all MGs. The proposed EMS is validated through five case studies using a test MMG network with six MGs, showing superior performance.

Many studies have been done in the field of MMG energy management due to increasing renewable energy sources in power systems, which creates increasing technical and

financial challenges. The future research directions in this field are recommended as follows:

1) In this study, a simple model is used to connect microgrids and form a MMG. In the future study, a more complex model can be used to better represent real cases.
2) Vehicle-to-grid (V2G) and grid-to-vehicle (G2V) can be used as resources.
3) To manage multi-uncertainties, different risk measures, such as Conditional Value-at-Risk (CVaR) and Glue-VaR, can be applied.

REFERENCES

[1] E. Fouladi, H. R. Baghaee, M. Bagheri, and G. B. Gharehpetian, "Power management of microgrids including PHEVs based on maximum employment of renewable energy resources," *IEEE Trans. Ind. Appl.*, vol. 56, no. 5, pp. 5299–5307, Sep. 2020.

[2] J. Guerrero, D. Gebbran, S. Mhanna, A. C. Chapman, and G. Verbič, "Towards a transactive energy system for integration of distributed energy resources: Home energy management, distributed optimal power flow, and peer-to-peer energy trading," *Renew. Sustain. Energy Rev.*, vol. 132, Oct. 2020, Art. no. 110000.

[3] M. Bornapour, R. Hemmati, M. Pourbehzadi, A. Dastranj, and T. Niknam, "Probabilistic optimal coordinated planning of molten carbonate fuel cell-CHP and renewable energy sources in microgrids considering hydrogen storage with point estimate method," *Energy Convers. Manage.*, vol. 206, Feb. 2020, Art. no. 112495.

[4] E. Bernardi, M. M. Morato, P. R. C. Mendes, J. E. Normey-Rico, and E. J. Adam, "Fault-tolerant energy management for an industrial microgrid: A compact optimization method," *Int. J. Electr. Power Energy Syst.*, vol. 124, Jan. 2021, Art. no. 106342.

[5] S. Chapaloglou, A. Nesiadis, K. Atsonios, N. Nikolopoulos, P. Grammelis, A. Carrera, and O. Camara, "Microgrid energy management strategies assessment through coupled thermal-electric considerations," *Energy Convers. Manage.*, vol. 228, Jan. 2021, Art. no. 113711.

[6] H. J. Kim, M. K. Kim, and J. W. Lee, "A two-stage stochastic P-robust optimal energy trading management in microgrid operation considering uncertainty with hybrid demand response," *Int. J. Electr. Power Energy Syst.*, vol. 124, Jan. 2021, Art. no. 106422.

[7] J. Faraji, H. Hashemi-Dezaki, and A. Ketabi, "Multi-year load growth-based optimal planning of grid-connected microgrid considering long-term load demand forecasting: A case study of Tehran, Iran," *Sustain. Energy Technol. Assessments*, vol. 42, Dec. 2020, Art. no. 100827.

[8] C.-S. Karavas, K. Arvanitis, and G. Papadakis, "A game theory approach to multi-agent decentralized energy management of autonomous polygeneration microgrids," *Energies*, vol. 10, no. 11, p. 1756, Nov. 2017.

[9] Y. Qiu, Q. Li, S. Zhao, and W. Chen, "Planning optimization for islanded microgrid with electric-hydrogen hybrid energy storage system based on electricity cost and power supply reliability," in *Renewable Energy Microgeneration Systems*. New York, NY, USA: Academic, 2021, pp. 49–67.

[10] M.-W. Tian and P. Talebizadehsardari, "Energy cost and efficiency analysis of building resilience against power outage by shared parking station for electric vehicles and demand response program," *Energy*, vol. 215, Jan. 2021, Art. no. 119058.

[11] M. Hu, F. Xiao, and S. Wang, "Neighborhood-level coordination and negotiation techniques for managing demand-side flexibility in residential microgrids," *Renew. Sustain. Energy Rev.*, vol. 135, Jan. 2021, Art. no. 110248.

[12] M. N. Gayathri, "A smart bidirectional power interface between smart grid and electric vehicle," in *Algorithms for Intelligent Systems*. Cham, Switzerland: Springer, 2021, pp. 103–137.

[13] V. Boglou, C. Karavas, A. Karlis, and K. Arvanitis, "An intelligent decentralized energy management strategy for the optimal electric vehicles' charging in low-voltage islanded microgrids," *Int. J. Energy Res.*, vol. 46, no. 3, pp. 2988–3016, Mar. 2022.

[14] Z. Wang, L. Chen, F. Liu, P. Yi, M. Cao, S. Deng, and S. Mei, "Asynchronous distributed power control of multimicrogrid systems," *IEEE Trans. Control Netw. Syst.*, vol. 7, no. 4, pp. 1960–1973, Dec. 2020.

[15] C. Klemm and P. Vennemann, "Modeling and optimization of multi-energy systems in mixed-use districts: A review of existing methods and approaches," *Renew. Sustain. Energy Rev.*, vol. 135, Jan. 2021, Art. no. 110206.

[16] H. Zou, S. Mao, Y. Wang, F. Zhang, X. Chen, and L. Cheng, "A survey of energy management in interconnected multi-microgrids," *IEEE Access*, vol. 7, pp. 72158–72169, 2019.

[17] V. Boglou, C. Karavas, A. Karlis, K. G. Arvanitis, and I. Palaiologou, "An optimal distributed RES sizing strategy in hybrid low voltage networks focused on EVs' integration," *IEEE Access*, vol. 11, pp. 16250–16270, 2023.

[18] H. Afrakhte and P. Bayat, "A contingency based energy management strategy for multi-microgrids considering battery energy storage systems and electric vehicles," *J. Energy Storage*, vol. 27, Feb. 2020, Art. no. 101087.

[19] N. M. Boopathi, "Marker-assisted selection," in *Genetic Mapping and Marker Assisted Selection*. New York, NY, USA: Academic, 2013, pp. 173–186.

[20] J. O. C. P. Pinto and M. Moreto, "Protection strategy for fault detection in inverter-dominated low voltage AC microgrid," *Electr. Power Syst. Res.*, vol. 190, Jan. 2021, Art. no. 106572.

[21] S. Nigam, O. Ajala, A. D. Domínguez-García, and P. W. Sauer, "Controller hardware in the loop testing of microgrid secondary frequency control schemes," *Electr. Power Syst. Res.*, vol. 190, Jan. 2021, Art. no. 106757.

[22] H. Qiu and F. You, "Decentralized-distributed robust electric power scheduling for multi-microgrid systems," *Appl. Energy*, vol. 269, Jul. 2020, Art. no. 115146.

[23] A. Bani-Ahmed, M. Rashidi, A. Nasiri, and H. Hosseini, "Reliability analysis of a decentralized microgrid control architecture," *IEEE Trans. Smart Grid*, vol. 10, no. 4, pp. 3910–3918, Jul. 2019.

[24] Q. Li, M. Gao, H. Lin, Z. Chen, and M. Chen, "MAS-based distributed control method for multi-microgrids with high-penetration renewable energy," *Energy*, vol. 171, pp. 284–295, Mar. 2019.

[25] Z. Zhao, J. Guo, C. S. Lai, H. Xiao, K. Zhou, and L. L. Lai, "Distributed model predictive control strategy for islands multimicrogrids based on noncooperative game," *IEEE Trans. Ind. Informat.*, vol. 17, no. 6, pp. 3803–3814, Jun. 2021.

[26] S. Leonori, A. Martino, F. M. Frattale Mascioli, and A. Rizzi, "Microgrid energy management systems design by computational intelligence techniques," *Appl. Energy*, vol. 277, Nov. 2020, Art. no. 115524.

[27] H. Karimi and S. Jadid, "Optimal energy management for multi-microgrid considering demand response programs: A stochastic multi-objective framework," *Energy*, vol. 195, Mar. 2020, Art. no. 116992.

[28] T.-C. Ou, "A novel unsymmetrical faults analysis for microgrid distribution systems," *Int. J. Electr. Power Energy Syst.*, vol. 43, no. 1, pp. 1017–1024, Dec. 2012.

[29] S. Jin, S. Wang, and F. Fang, "Game theoretical analysis on capacity configuration for microgrid based on multi-agent system," *Int. J. Electr. Power Energy Syst.*, vol. 125, Feb. 2021, Art. no. 106485.

[30] M. Ahrabi, M. Abedi, H. Nafisi, M. A. Mirzaei, B. Mohammadi-Ivatloo, and M. Marzband, "Evaluating the effect of electric vehicle parking lots in transmission-constrained AC unit commitment under a hybrid IGDT-stochastic approach," *Int. J. Electr. Power Energy Syst.*, vol. 125, Feb. 2021, Art. no. 106546.

[31] H. Khaloie, A. Abdollahi, M. Shafie-Khah, P. Siano, S. Nojavan, A. Anvari-Moghaddam, and J. P. S. Catalão, "Co-optimized bidding strategy of an integrated wind-thermal-photovoltaic system in deregulated electricity market under uncertainties," *J. Cleaner Prod.*, vol. 242, Jan. 2020, Art. no. 118434.

[32] S. Li, J. Zhu, Z. Chen, and T. Luo, "Double-layer energy management system based on energy sharing cloud for virtual residential microgrid," *Appl. Energy*, vol. 282, Jan. 2021, Art. no. 116089.

[33] S. Kaur, L. K. Awasthi, A. L. Sangal, and G. Dhiman, "Engineering applications of artificial intelligence tunicate swarm algorithm: A new bio-inspired based metaheuristic paradigm for global optimization," *Eng. Appl. Artif. Intell.*, vol. 90, Apr. 2020, Art. no. 103541.

[34] J. Gao, J. J. Chen, B. X. Qi, Y. L. Zhao, K. Peng, and X. H. Zhang, "A cost-effective two-stage optimization model for microgrid planning and scheduling with compressed air energy storage and preventive maintenance," *Int. J. Electr. Power Energy Syst.*, vol. 125, Feb. 2021, Art. no. 106547.

[35] Y.-C. Tsao and V.-V. Thanh, "Toward blockchain-based renewable energy microgrid design considering default risk and demand uncertainty," *Renew. Energy*, vol. 163, pp. 870–881, Jan. 2021.

[36] M. Moradi-Dalvand, B. Mohammadi-Ivatloo, N. Amjady, H. Zareipour, and A. Mazhab-Jafari, "Self-scheduling of a wind producer based on information gap decision theory," *Energy*, vol. 81, pp. 588–600, Mar. 2015.
[37] E. Maibach, J. Miller, F. Armstrong, O. El Omrani, Y. Zhang, N. Philpott, S. Atkinson, L. Rudoph, J. Karliner, J. Wang, C. Pétrin-Desrosiers, A. Stauffer, and G. K. Jensen, "Health professionals, the Paris agreement, and the fierce urgency of now," *J. Climate Change Health*, vol. 1, Mar. 2021, Art. no. 100002.
[38] M. Parol, T. Wójtowicz, K. Ksiezyk, C. Wenge, S. Balischewski, and B. Arendarski, "Optimum management of power and energy in low voltage microgrids using evolutionary algorithms and energy storage," *Int. J. Electr. Power Energy Syst.*, vol. 119, Jul. 2020, Art. no. 105886.
[39] P. Ornetti, C. Fortunet, C. Morisset, V. Gremeaux, J. F. Maillefert, J. M. Casillas, and D. Laroche, "Clinical effectiveness and safety of a distraction-rotation knee brace for medial knee osteoarthritis," *Ann. Phys. Rehabil. Med.*, vol. 58, no. 3, pp. 126–131, Jun. 2015.
[40] J. Liu, X. Chen, Y. Xiang, D. Huo, and J. Liu, "Optimal planning and investment benefit analysis of shared energy storage for electricity retailers," *Int. J. Electr. Power Energy Syst.*, vol. 126, Mar. 2021, Art. no. 106561.
[41] T. Adefarati, R. C. Bansal, M. Bettayeb, and R. Naidoo, "Optimal energy management of a PV-WTG-BSS-DG microgrid system," *Energy*, vol. 217, Feb. 2021, Art. no. 119358.
[42] S. Mirmohammadi, J. Yazdani, S. Etemadinejad, and H. Asgarinejad, "A cross-sectional study on work-related musculoskeletal disorders and associated risk factors among hospital health cares," *Proc. Manuf.*, vol. 3, pp. 4528–4534, Jul. 2015.
[43] J. Faraji, H. Hashemi-Dezaki, and A. Ketabi, "Stochastic operation and scheduling of energy hub considering renewable energy sources' uncertainty and N-1 contingency," *Sustain. Cities Soc.*, vol. 65, Feb. 2021, Art. no. 102578.
[44] A. K. Karmaker, M. M. Rahman, M. A. Hossain, and M. R. Ahmed, "Exploration and corrective measures of greenhouse gas emission from fossil fuel power stations for Bangladesh," *J. Cleaner Prod.*, vol. 244, Jan. 2020, Art. no. 118645.
[45] A. Miskelly. (2021). *Wind Turbine Output Power*. [Online]. Available: https://anero.id/energy/data
[46] (2021). *Free Online Service for Sharing and Comparing Photovoltaic Solar Panel Output Data*. [Online]. Available: https://pvoutput.org/live.jsp
[47] A. Arefi and F. Shahnia, "Tertiary controller-based optimal voltage and frequency management technique for multi-microgrid systems of large remote towns," *IEEE Trans. Smart Grid*, vol. 9, no. 6, pp. 5962–5974, Nov. 2018.
[48] S. Kaur, L. K. Awasthi, A. L. Sangal, and G. Dhiman, "Tunicate swarm algorithm: A new bio-inspired based metaheuristic paradigm for global optimization," *Eng. Appl. Artif. Intell.*, vol. 90, Sep. 2020, Art. no. 103541.

REZA RASHIDI was born in Kermanshah, Iran, in 1984. He received the M.Sc. degree in electrical engineering from the Science and Research Branch, Tehran, Iran, in 2015, and the Ph.D. degree in electrical engineering from Bu-Ali Sina University, Hamedan, Iran, in 2022. His research interests include operation, transmission expansion planning, renewable energies, smart grids, microgrids, the energy management of microgrids, power grids stability, and the design of electrical and control systems for industrial plants.

ALIREZA HATAMI received the B.Sc. degree in electrical engineering from the Amirkabir University of Technology, Tehran, Iran, in 1995, and the M.Sc. and Ph.D. degrees from Tarbiat Modares University, Tehran, in 1998 and 2009, respectively. He is currently an Associate Professor of electrical engineering with Bu-Ali Sina University, Hamedan, Iran. His research interests include energy management, smart grids, and risk modeling.

MANSOUR MORADI was born in Eslamabad Gharb, Iran, in 1987. He received the B.Sc. degree in electrical engineering from Islamic Azad University (IAU), Brojerd Branch, Iran, in 2010, and the M.Sc. degree in electrical engineering from IAU, Science and Research Branch, Tehran, Iran, in 2013. He is currently a Lecturer with the Electrical Engineering Department, Technical and Vocational University (TVU), Kermanshah, Iran. His research interests include power system optimization, operation and planning, transmission expansion planning (TEP), renewable energies, smart grids, microgrids, uncertainty modeling, evolutionary optimization algorithms, artificial intelligence, data mining, machine learning, and deep learning.

XIAODONG LIANG (Senior Member, IEEE) was born in Lingyuan, Liaoning, China. She received the B.Eng. and M.Eng. degrees in electrical engineering from Shenyang Polytechnic University, Shenyang, China, in 1992 and 1995, respectively, the M.Sc. degree in electrical engineering from the University of Saskatchewan, Saskatoon, Canada, in 2004, and the Ph.D. degree in electrical engineering from the University of Alberta, Edmonton, Canada, in 2013.

From 1995 to 1999, she was a Lecturer with Northeastern University, Shenyang. In October 2001, she joined Schlumberger (SLB), Edmonton, and was promoted to the Principal Power Systems Engineer with this world's leading oil field service company, in 2009. She was with Schlumberger for almost 12 years, until August 2013. From 2013 to 2019, she was with Washington State University, Vancouver, WA, USA, and the Memorial University of Newfoundland, St. John's, NL, Canada, as an Assistant Professor and later an Associate Professor. In July 2019, she joined the University of Saskatchewan, where she is currently a Professor and Canada Research Chair in Technology Solutions for Energy Security in Remote, Northern, and Indigenous Communities. She was an Adjunct Professor with the Memorial University of Newfoundland, from 2019 to 2022. Her research interests include power systems, renewable energy, and electric machines.

Dr. Liang is a Registered Professional Engineer of Saskatchewan Province, Canada; a fellow of IET; and the Deputy Editor-in-Chief of IEEE TRANSACTIONS ON INDUSTRY APPLICATIONS.